

# Accepted Manuscript

Research paper

Encapsulated Schiff Base Nickel Complex in Zeolite Y: Correlation Between Catalytic Activities and Extent of Distortion Supported by Experimental and DFT Studies

Archana Choudhary, Bidisa Das, Saumi Ray

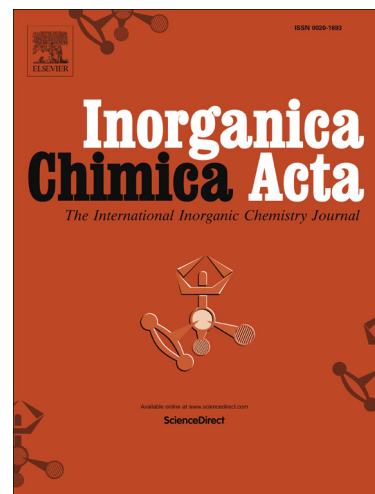
PII: S0020-1693(17)30186-X  
DOI: <http://dx.doi.org/10.1016/j.ica.2017.04.003>  
Reference: ICA 17507

To appear in: *Inorganica Chimica Acta*

Received Date: 8 February 2017  
Revised Date: 31 March 2017  
Accepted Date: 3 April 2017

Please cite this article as: A. Choudhary, B. Das, S. Ray, Encapsulated Schiff Base Nickel Complex in Zeolite Y: Correlation Between Catalytic Activities and Extent of Distortion Supported by Experimental and DFT Studies, *Inorganica Chimica Acta* (2017), doi: <http://dx.doi.org/10.1016/j.ica.2017.04.003>

This is a PDF file of an unedited manuscript that has been accepted for publication. As a service to our customers we are providing this early version of the manuscript. The manuscript will undergo copyediting, typesetting, and review of the resulting proof before it is published in its final form. Please note that during the production process errors may be discovered which could affect the content, and all legal disclaimers that apply to the journal pertain.



**Encapsulated Schiff Base Nickel Complex**  
**in Zeolite Y: Correlation Between Catalytic Activities and Extent of Distortion Supported by**  
**Experimental and DFT Studies**

Archana Choudhary<sup>a</sup>, Bidisa Das<sup>b</sup> and Saumi Ray<sup>\*a</sup>

<sup>a</sup>Birla Institute of Technology and Science, Pilani, Rajasthan 333031

<sup>b</sup>Indian Association for the Cultivation of Science, Jadavpur, Kolkata 700032.

**ABSTRACT:** It is observed that planar Ni (II)–Schiff base complexes of general formulae NiL with L as N, N'-bis(4-hydroxy salicylidene)ethylenediamine (4-OH-salen) when encapsulated in the supercage of zeolite Y, the complex adopts non-planar geometry. The detailed characterization studies of the 4-OH-Ni-salen complex when compared with Ni-salen complex encapsulated in zeolite Y (Ni-salen-Y)[1] have suggested that the complex undergoes more distortion in order to accommodate itself inside the supercage of zeolite-Y. Optical spectroscopic studies show relatively more blue shifted and intensified d-d transition for 4-OH-Ni-salen complex after encapsulation. We also report the catalytic activities and enhanced magnetization of encapsulated complex though it is diamagnetic in the 'free' state. DFT studies of these complexes have been carried out in different spin states and electronic spectra are simulated to have better insight about the geometries adopted by the guest complexes inside the host framework.

## INTRODUCTION

Zeolites are microporous materials having three dimensional long ranges ordered aluminosilicate framework with the channels and cavities of precise and regular size [2-6]. These materials have numerous applications in petrochemical industries [7-9] and is utilized as potential shape and size selective heterogeneous catalysts [10, 11] for wide range of the chemical reactions. The fascinating architecture of zeolite helps to design coupled systems by encapsulating organic, inorganic molecules, clusters, dyes and nanoparticles inside the cavities of the host lattice so that these coupled materials can have diverse applications [12-18]. Additionally, they are thermally stable with varied active sites and act as eco-friendly medium for different processes. They are also known as 'solid acid' due to the presence of Brønsted and Lewis acid sites and even can be used like sulphuric acid in the chemical reactions [19-21]. The encapsulated transition metal complexes like phthalocyanine, bipyridyl and Schiff base ligands in zeolites are well recognized as bio mimetic systems and are known as 'zeozymes' as they have shown the structural and functional analogy with the metallo-enzymes such as cytochrome 450 [22, 23]. These heterogeneous systems offer a novel route to couple the reactivity of metal complex with special structural robustness of zeolites. The systems, where the complex is synthesized inside the cavity of zeolite, cannot escape out of the supercage due to size restriction of the window, are especially known as 'ship-in-a-bottle' complexes [24]. The modified catalytic activity and selectivity of the encapsulated complexes originates from host-guest interaction in the hybrid system. Rudy F. Patron et al reported that iron phthalocyanine complex in zeolites Y is a mimic of cytochrome 450 and 10 times more efficient for oxidation of C-H bond in mono branched hydrocarbons. The authors have reported that zeolite framework exercises the steric constraint on active site of FePc complex as does the protein mantle in cytochrome 450. In another report P.A. Jacob et.al have reported that the manganese complexes in zeolites X and Y are selective towards alkenes oxidation reactions [25]. The zeolite encapsulated metal Schiff-base complexes are well explored as catalysts for the various reactions like oxidation of toluene, benzyl alcohol, cyclohexane, ethyl benzene methyl phenyl sulphide, and styrene [26-33], with mild oxidants like H<sub>2</sub>O<sub>2</sub> and TBHP. A recent report has also explored the other dimensions of these systems and found

that the amine functionalized ionic liquid encapsulated in zeolites Y shows capability for CO<sub>2</sub> capture [34]. Catalysis of zeolite encapsulated complexes is well investigated research area however the impact of encapsulation on the structural alteration of the guest complex still remains relatively less studied, though the enhanced selectivity and modified reactivity might have strong correlation with altered geometry adopted by the encapsulated complex. There are only few reports available in the literature [35-38], which have explored the influence of the topology of the void on the geometry of encapsulated complex and its consequences in terms of change in electronic, physical, catalytic and redox properties of encapsulated system. A series of Fe<sup>2+</sup> complexes with different ligands encapsulated in zeolite Y, have been reported and with the help of spectroscopic techniques it is observed that the smaller complexes like [Fe(en)<sub>3</sub>]<sup>2+</sup> and [Fe(amp)<sub>3</sub>]<sup>2+</sup> stay inside the supercage without any distortion, but complexes with slightly larger size with respect to the zeolite cavity like [Fe(bpy)<sub>3</sub>]<sup>2+</sup> and [Fe(phen)<sub>3</sub>]<sup>2+</sup>, have adopted significantly distorted geometry on encapsulation, and further attempt to encapsulate bigger complexes like [Fe(dmbpy)<sub>3</sub>]<sup>2+</sup> and [Fe(dmphen)<sub>3</sub>]<sup>2+</sup> is a failure. In other report, exciting magnetic behaviour of encapsulated complex has been observed where authors have reported that the [Co(bpy)<sub>3</sub>]<sup>2+</sup> complex after encapsulation in zeolite Y shows the temperature driven spin crossover phenomena, whereas the complex ion in its free form retains a high spin ground state in solution as well as in solid state [37]. Ray et al have reported that the square planar cobalt phthalocyanine of D<sub>4h</sub> symmetry, under encapsulation in zeolites Y, adopts a distorted geometry and as a result encapsulated complex shows altered magnetic behaviour with enhanced magnetic moment [35]. R.C. Deka et al have observed that cobalt phenanthroline complex after encapsulation in zeolites Y exhibits difference in electrochemical response and shifted positions of frontier orbitals of the molecule, further explored by DFT studies [38]. Earlier we have reported that the diamagnetic nickel Schiff-base complex when encapsulated in zeolite Y, adopts the non-planar geometry due to space constraint where nickel metal is out of the plane of N<sub>2</sub>O<sub>2</sub> moiety, exhibiting paramagnetism, however the same complex, when encapsulated in another host with much larger pore diameter such as MCM-41, doesn't show this behaviour [39]. Recently it is observed that the nickel (II) Schiff-base complexes having different molecular dimensions when encapsulated within the zeolite supercage, higher

the molecular dimension, greater are the degree of distortion of the structure of the encapsulated complex and the catalytic activity [1]. In the present manuscript, we report the encapsulation of the 4-OH nickel Schiff base complex with nearly same 'end to end' distance ( $\sim 12.98 \text{ \AA}$ ) of nickel salen complex [1] encapsulated within the supercage of zeolite-Y with a pore diameter of  $12.47 \text{ \AA}$  via flexible ligand synthesis method. The difficulty therefore lies in how to fit the planar complex into the spherical cavities. We have carried out the detailed characterization of the system with the help of comparative spectroscopic (IR, UV-Vis), morphological (XRD, SEM), magnetic and theoretical studies to understand the confinement of the complex in zeolite Y supercage. DFT studies have provided the detailed information of different adopted geometries of the guest complexes under space constraint within zeolite. Furthermore, optical spectra are simulated employing TD-DFT method to have a greater insight of the experimentally observed shifts in UV-Vis spectra of the zeolite encapsulated complexes. Additionally, we have employed complex as catalyst both in free and entrapped states on the styrene oxidation reaction to comprehend the extent of distortion and modified reactivity of the complexes after encapsulation in zeolite Y.

## RESULT AND DISCUSSIONS

### Powder XRD Analysis

The powder X-ray diffraction patterns of Na-zeolite Y, Ni-zeolite Y, and 4-OH-Ni-salen complex in zeolite Y (4-OH-Ni-salen-Y) systems are shown in Figure 1. The powder XRD pattern of 4-OH-Ni-salen-Y is essentially similar with that of the pure and nickel exchanged zeolite Y, indicating the retention of integrity of host zeolite lattice after the encapsulation processes. However a noticeable intensity reversal is observed at  $2\theta = 10^\circ$  and  $12^\circ$  positions in the XRD patterns for the encapsulated complex. Pure and nickel exchanged zeolite Y hold the intensities relation as  $I_{220} > I_{311}$ , but after the encapsulation of complex in the supercage, the XRD pattern of the hybrid system holds the reverse relation of intensities as  $I_{220} < I_{311}$ . In the literature, empirical correlation of such observation with the presence of a large complex inside the supercage of zeolite Y already exists.[40-43] Similar observation in XRD patterns is observed for the nickel salen-Y complex [1]. Such type of experimental observation does not appear in case of tethering

of complex and even if complex does not form in the cavity of supercage [38, 44]; XRD experimental data suggest the encapsulation of guest complex is successfully carried out in the pores of zeolite. Appearance of any extra peak is not observed as expected because the loading levels of the metal complex maintained in zeolite are very low.

### Elemental Analysis

The parent host material, Na-zeolite Y has the unit cell formula as  $\text{Na}_{58}\text{Al}_{58}\text{Si}_{136}\text{O}_{388}\cdot y\text{H}_2\text{O}$  and Si/Al ratio is 2.34. EDS spectra and data of 4-OH-Ni-salen-Y [supporting information Figure S1] suggests that Si/Al ratio (2.30) remains unaffected in encapsulated complex, which signifies that the leaching of aluminium doesn't take place during encapsulation processes. Presence of both the sodium and nickel metal ions, in the hybrid system of zeolite with the encapsulated complex within indicates the partial exchange of sodium metal ions during exchange reactions. The nickel ion concentration in encapsulated complex is observed to be lesser (0.50 wt %) than that in nickel exchanged zeolite Y (0.92 wt %) as expected because of possible leaching of some of the metal ions during the synthesis of complex which in turn, can lead in lowering the nickel ion concentration.

### Scanning Electron Microscopy Analysis

Encapsulation of metal complex within the supercage of zeolite-Y essentially targets the complex formation only inside the cavities of supercage, however such a precise method of synthesis not feasible practically. Inevitable adsorptions of some complexes and ligand on the surface of zeolite lattice have been removed by extensive Soxhlet extraction. SE micrographs of pure zeolite Y, 4-OH-Ni-salen -Y after Soxhlet extraction is shown (Figure 2 a-b). After Soxhlet extraction, surface boundaries of host lattice are much clearly visible and differentiable, providing a clear indication of the removal of surface species from surface, as well as preservation of crystallinity of zeolite framework [42, 45]. Eventually the SEM analysis gives the indirect evidence about the complex formation, mostly occurring inside the host cavity only.

### X-Ray Photoelectron Spectroscopy

The existence of metal complex in the zeolite framework has been further confirmed by the X-ray photoelectron spectroscopy (XPS). The survey spectra and high resolution XP spectra of C (1s), N (1s), O (1s) and Ni (2p) of 4-OH-Ni-salen-Y are presented in Figure 3. The observed spectra and binding energy data (Figure 3 and Table 1) clearly indicates the presence of C, N, O, Na, Si, Al, Ni(II) in their respective chemical states, which is accordance to the literature [1, 46-50]. The loading level of metal is low in the complex within the host lattice, therefore the weak XPS peak intensities are observed for nickel (2p) signals for the encapsulated complex (4-OH-Ni-salen-Y) and it is perfectly in agreement with the other concentration dependent studies obtained from EDX, IR and UV-Visible spectroscopies. It already has been observed that Ni-salen in both its free and zeolite encapsulated forms show the appearance of  $2p_{3/2}$  and  $2p_{1/2}$  peaks in the XPS spectra at the binding energies at around 855 and 872 eV suggesting nickel metal present in +2 oxidation state in both the forms [1]. As well as absence of any shake up and satellite peak around 878 eV confirms that the complex stays in square planar geometry not in the octahedral geometry [46, 49]. Intense and broad carbon (1s) XPS spectra have observed for nickel salen complex in both states which further deconvoluted into two peaks and validated the presence of  $sp^3$  and  $sp^2$  carbon atoms in complex. Similarly the complex have shown the nitrogen (1s) and oxygen (1s) XPS traces for (M-N), (N=C) and (C-O), (M-O) respectively [1]. In the present study, encapsulated 4-OH-Ni-salen-Y also has shown the essentially similar patterns of XPS signals for all constituent atoms of the complex with the minor shifts in the signals. The encapsulated 4-OH-Ni-salen complex has demonstrated  $2p_{3/2}$  and  $2p_{1/2}$  peaks at 853.40 and 872.95 eV binding energies since Ni in the complex is present in +2 oxidation state with square planar geometry. Furthermore, carbon (1s) XPS spectra of 4-OH-Ni-salen-Y have confirmed the presense of  $sp^3$  and  $sp^2$  carbon atoms and XPS traces of nitrogen (1s) are deconvoluted into two signals associated to (M-N) and (N=C) peaks. Oxygen (1s) XPS traces are deconvoluted into two peaks which are attributed to (M-O) and (C-O) peaks. All observed signals along with the Si (2p) and Al (2p) peaks in 4-OH-Ni-salen-Y hybrid system are in accordance with the literature [1]. Presence of all

elements in the expected chemical states and nickel metal ion in +2 oxidations state undeniably signifies the successful formation of 4-OH-Ni-salen complex within the supercage of zeolite-Y.

### Infrared Spectroscopy

The IR spectra of pure zeolite Y, 4-OH-Ni-salen, and 4-OH-Ni-salen-Y are shown in Figure 4, and corresponding data are provided in the Table 2. Pure-zeolite-Y mainly shows bands in the region of 450-1200  $\text{cm}^{-1}$  and also at around 1643  $\text{cm}^{-1}$  and 3500  $\text{cm}^{-1}$  region. The major characteristics bands at 560, 717, 786, and 1018  $\text{cm}^{-1}$  are identified as (Si/Al-O)<sub>4</sub> bending mode, double ring, symmetric stretching and asymmetric stretching vibration respectively [51]. Another two broad bands at 3500  $\text{cm}^{-1}$  and 1643  $\text{cm}^{-1}$  are originated from the surface hydroxylic group and lattice water molecules respectively [45]. The appearance of these bands even for the integrated host-guest systems (Figure 4) indicates the preservation of host lattice integrity, during the process of encapsulation. However, the characteristic IR bands of the encapsulated complexes are majorly masked by strong zeolitic bands over most of the range. The signal intensity is very low, because of very low concentration of metal complex inside the framework, the only region of 1600-1200  $\text{cm}^{-1}$  is found to be suitable for the study because in that region bands appear only from the guest complex.; Within 1600-1200  $\text{cm}^{-1}$ , encapsulated complex shows main characteristics C=C, C=N and C-O stretching [52] and C-H deformation bands with small shifts. The shift in these bands can be due to the different environment imposed by the cavity on the of guest complex. The C-H deformation band of the complex has shifted from 1375  $\text{cm}^{-1}$  to 1381  $\text{cm}^{-1}$  under encapsulation [1, 53]. These observed IR data point towards the successful synthesis of the nickel Schiff-base complex inside the pores of zeolite-Y. The overall experimental FTIR spectral data (Table 2) suggests the successful synthesis of the complex in the 'free' as well as in encapsulated state inside the zeolite Y cavities.

### UV-Visible Spectroscopy

Electronic spectra of the 4-OH-salen ligand and 'free state' 4-OH-Ni-salen complex have been recorded in

chloroform (supporting information, Figure S2). Chloroform is preferred over the other solvents because it is already an established fact that in chloroform, such complexes experience minimum structural deviation from planarity when dissolved in chloroform [39, 54]. The comparative solid state UV-Vis studies of the complex in 'free state' complex and zeolite entrapped state have been carried out (shown in Figure 5 and Table 3) to explore the change of electronic environment around the metal centre after encapsulation. Not only that, comparative studies of this system with those of Ni-salen become relevant in this point to investigate the effect of the substituent groups. The free state complexes Ni-salen (Figure 5a), 4-OH-Ni-salen (Figure 5b) show the high energy strong bands at 251 nm and 241 nm respectively, which are attributed to  $\pi-\pi^*$  transitions. Further two bands at 323 and 413 nm in the spectrum of Ni-salen, and at 325 nm and 397 nm in the spectrum of 4-OH-Ni-salen are the  $n-\pi^*$  transitions [1, 45]. For both Ni-salen and 4-OH-Ni-salen, relatively weak yet broad absorption bands adjacent to  $n-\pi^*$  bands, at 453 nm and 439 nm respectively must have originated from charge transfer transitions. The broad d-d band centered at  $\sim(555-570)$  nm for Ni-salen [1] and  $\sim(560-580)$  nm for 4-OH-Ni-salen can be attributed majorly to the transition from  $d_z^2$  to  $d_{xy}$  orbital [55]. The appearance of charge transfer bands and d-d bands directly proves the formation of the complex. The UV-Vis spectral bands of encapsulated complexes are not so distinctly visible, due to very low concentration of complex inside zeolite, but it is quite apparent that, the high energy  $\pi-\pi^*$  and  $n-\pi^*$  transitions for both the encapsulated complexes Ni-salen-Y (Figure 5d), 4-OH-Ni-salen-Y (Figure 5c) secure nearly same positions as their corresponding 'free state' complexes. However on encapsulation, lower energy d-d bands, are considerably intensified [53] and blue shifted [1, 39] with respect to the corresponding 'free state' d-d bands. Such type of electronic behaviour reveals that the complex is not able to sustain its planar geometry especially around the metal ion due to space restrictions imposed by the host cavity. Though both Ni-salen and 4-OH-Ni-salen complexes have nearly same end-to-end distances as 12.94 Å and 12.99 Å respectively, two hydroxyl substituent's on both the benzene rings of 4-OH-Ni-salen complex lead in increase of the width of the complex essentially requiring more space to be accommodated inside the nearly spherical supercage (cavity diameter is 12.47Å). The extent of observed blue shift in d-d bands is roughly double

for 4-OH-Ni-salenas compared to that of Ni-salen under entrapment. The observed blue shift in the d-d band of Ni-salen-Y is around 30 nm, whereas that in 4-OH-Ni-salen-Y is approximately 60 nm. The observed blue shift definitely in turn points towards the reduction of the gap between  $d_{xy}$  and  $d_{x^2-y^2}$  orbitals. This observation is in line with the argument that extent of distortion in the case of entrapped 4-OH-Ni-salen complex is more than that for Ni-salen complex under confinement. It is explicable, as the complex with comparatively bulkier ligand experiences more space constraint, imposed by the host framework, which makes the complex more distorted and is also well supported by the electronic spectroscopic studies.

## Theoretical Studies & Results

### Structure & Geometry

The ground states of Ni-salen and 4-OH-Ni-salen complexes are planar, diamagnetic and exist as singlet states without any unpaired electrons (The details of theoretical studies on Ni-salen and 4-OH-Ni-salen complexes in isolated, singlet and encapsulated triplet forms are discussed in SI section). The structure of the Ni-salen and 4-OH-Ni-salen complexes in the free state and then in zeolite encapsulated triplet states are relaxed and the optimized structures are presented in Figure 6. The structure of the encapsulated complexes shows deviations from those of the neat complexes and few important results have been tabulated in Table 4. The variations in the bond distances and bond angles upon encapsulation are small and are due to the influence of the zeolite framework, however, the Ni-salen/4-OH-Ni-salen complexes as a whole are deformed and puckered when packed inside the pore. The encapsulation process changes the ordering of the molecular orbitals in such a way that the magnetic triplet state becomes stable. The switching of a diamagnetic planer molecule to a magnetic puckered molecule when encapsulated is the focus of the present work.

The neat Ni-salen and 4-OH-Ni-salen complexes though are planar, diamagnetic and are more stable in singlet states, they may also exist in high energy triplet states with two unpaired electrons. The energy differences calculated between the singlet state and the triplet state for free neat Ni-salen is 12.8 kcal and

11.8 kcal for 4-OH-Ni-salen. The non planer triplet state predominates when encapsulated as the experimental magnetic studies indicate. The theoretical spin densities on Ni atom is 1.56 (total moment: 2.35 BM,  $[n(n+2)]^{1/2}$ , where n is number of unpaired electrons) for Ni-salen and 1.68 (total moment: 2.49 BM) for 4-OH-Ni-salen. From the results tabulated in Table 3, we find that Ni-N distances change from 1.87 Å for the neat complexes to 1.96 Å for the encapsulated complexes and Ni-O distances change from ~1.86 Å in neat states to ~1.89 Å when encapsulated both for Ni-salen and 4-OH-Ni-salen. The O-C and N-C distances are 1.29 Å for both free and encapsulated cases of Ni-salen and 4-OH-Ni-salen. The O-Ni-N bond angle decreases from 93.9° to 92.3° and the angle C-Ni-C (atoms shown in rectangular boxes as marked in Figure 6, give an idea about the non-planarity of the molecule), changes from 179.99° to 169.7° in case of the Ni-salen after encapsulation. The HOMO for neat Ni-salen has a  $d_{yz}$  character hybridized with the p bonding character of the salen ligand, and the LUMO has Ni  $d_{xz}$  character hybridised with p antibonding type orbitals from C and N. The HOMO and LUMO energies are -5.28 and -1.83 eV respectively with a HOMO-LUMO energy gap of 3.45 eV. The overall distortion of the complex 4-OH-Ni-salen after encapsulation is indicated from the same bond-angles O-Ni-N; which changes from 93.9° to 92.2° and C-Ni-C which changes from 179.99° to 169.3°. The HOMO for the isolated 4-OH-Ni-salen complex has a  $d_{yz}$  character and the LUMO has Ni  $d_{xz}$  character. The HOMO and LUMO energies are -5.26 and -1.60 eV respectively with a HOMO-LUMO energy gap of 3.66 eV. The change in the bond distances and bond angles on encapsulation may be attributed to the influence of the zeolite framework, where the zeolite valence electrons are distributed all over as a delocalized electron cloud and interacts strongly with the encapsulated Ni complex.

#### Optical transitions from TD-DFT studies

TD-DFT methods are employed to calculate the UV-Vis spectra for the singlet states of the neat complexes and triplet spin states for the encapsulated Ni-salen and 4-OH-Ni-salen complexes, as given in Figure 7. In case of isolated Ni-salen, the d-d transition is calculated at 633 nm, a transition from HOMO orbital (Ni  $d_{yz}$ ) to LUMO+2 (Ni  $d_{xy}$  hybridized with O and N p orbitals). The transition around 555 nm occurring from HOMO-2 (Ni  $d_z^2$ ) to LUMO+2 (Ni  $d_{xy}$ ) is also a d-d transition. Another d-d transition is

calculated at 493 nm which is HOMO-3 (Ni  $d_{yz}$ ) to LUMO+2 (Ni  $d_{xy}$ ), but it is hybridized with ligand orbitals. Strong bands around 420 and 350 nm are due to transitions; HOMO to LUMO+1, HOMO-2 to LUMO and HOMO-1 to LUMO respectively which could correspond to the  $n-\pi^*$  bands as observed experimentally. Several intra ligand charge transfer bands ( $\pi-\pi^*$ ) are calculated around 280 nm. For encapsulated Ni-salen-Y complex, the d-d transition appears at 589 nm which is a transition from HOMO-6 orbital (Ni  $d_z^2$ ) to LUMO+3 orbital (Ni  $d_{xy}$ ). Next moderately intense transition is observed at 499 nm which is HOMO-1 to LUMO transition and is a ligand to metal charge transfer transition. The intense transitions occurring at 450-390 nm (HOMO to LUMO, HOMO-1 to LUMO, HOMO to LUMO+1 orbitals) are primarily intra ligand transitions with minimal involvement of metal d orbitals and correspond to  $n-\pi^*$  bands experimentally.

In case of isolated 4-OH-Ni-salen complex, the d-d transitions are found at 627 nm, a transition from HOMO (Ni  $d_{yz}$ ) to LUMO+2 (Ni  $d_{xy}$  hybridized with O and N p orbitals) and at 556 nm from HOMO-4 (Ni  $d_z^2$ ) to LUMO+2 (Ni  $d_{xy}$ ). Ligand to metal charge transfer transition is calculated at 451 nm (HOMO-5 to LUMO+2) and at 396 nm the transition from HOMO to LUMO+1 is an intra ligand transition. Strong transitions around 340-310 nm are  $n-\pi^*$  transitions. Several  $\pi-\pi^*$  bands occur around 270 nm. For encapsulated 4-OH-Ni-salen complex, the d-d transition appears at 596 nm which is a transition from HOMO-6 orbital (Ni  $d_z^2$ ) to LUMO+3 orbital (Ni  $d_{xy}$  hybridized with O and N p orbitals). Moderately intense transitions are observed at 475, 462 nm which are HOMO-1 to LUMO and HOMO-4 to LUMO+3 for beta orbitals, which are mainly ligand to metal charge transfer transition. Theoretically there are intense transitions occurring at 350-320 nm are primarily intra ligand transitions with very small involvement of metal d orbitals. Theoretically intense  $\pi-\pi^*$  intra ligand transitions occur around 270-290 nm for both complexes.

From the theoretical study of optical transitions, it is clear that after encapsulation, the d-d transition is shifted to lower wavelengths for both complexes by 30-40 nm, but the  $n-\pi^*$  and the  $\pi-\pi^*$  transitions remain largely unaltered, similar to experimental observations. It is important to note that the observed d-

d shifts in the spectra of encapsulated complexes have major contributions from  $d_z^2$  and  $d_{xy}$  atomic orbitals of Ni as expected for square planer complexes. DFT study also reveals that every transition associated with the  $d_{xy}$  orbital is essentially blue shifted, which points towards the reducing energy gap between the  $d_{xy}$  and  $d_z^2$  orbitals and slightly higher lying triplet state becomes comparatively more accessible which also leads to a significant increase in the magnetic moment after encapsulation.

### Magnetic Studies

Optical spectroscopic studies as well as the theoretical studies clearly indicate the distortion in geometry of 4-OH-Ni-salen complex upon encapsulation, therefore to comprehend the geometry adopted by the encapsulated complex especially around the metal centre, magnetic studies have been carried out and then compared with that of Ni-Salen (without any substitution) entrapped in zeolite-Y [1]. As mentioned in elemental analysis section, the loading level of nickel in 4-OH-Ni-salen-Y is 0.50 wt % whereas in Ni-salen-Y is 0.59 wt %. The planar  $d^8$  nickel complexes are diamagnetic. Several literature reports are available, which clearly suggest that these metal complexes are diamagnetic in nature, without any effect of the substituent on the benzene rings [56-58]. From the observed experimental magnetic data in the temperature range of 4K-300K, the Ni-salen complex, is found to be almost diamagnetic with magnetic moment near to zero (0.45 BM), which essentially indicate planarity of  $N_2O_2$  moiety around the Ni(II) centre [1, 56]. However, in the same temperature range, both the encapsulated 4-OH-Ni-salen and Ni-salen complexes display markedly different behaviour. The plots of molar susceptibility vs., temperature (5-300) K for both the encapsulated complexes along with that of the neat Ni-salen are shown in Figure 8. The origin of such radically different behavior of the hybrid system is apparently from the guest nickel complexes, as the host is diamagnetic [40, 59]. On the other hand, the paramagnetic behaviors of the encapsulated Ni complexes are quite evident. This enhanced paramagnetism must be instigated from the structural deformation of the encapsulated complex where Ni ion experiences an electronic environment different from that of the neat complex, and the non-planar  $NiN_2O_2$  moiety results in an altered ordering of molecular energy levels. As a result, the slightly higher lying excited triplet state becomes

comparatively more accessible. This argument is even strongly supported by the theoretical studies and experimentally obtained optical data indicating the fact that encapsulation causes significant reduction of the energy gap between the highest lying metal  $d_{x^2-y^2}$  and next highest  $d_{xy}$  orbitals. Hence encapsulation enables a considerable fraction of the complex molecules to exist in high energy triplet states and is consequently responsible for the substantial increase in the magnetization of the encapsulated complex.

Comparing the magnetic behaviour of both the encapsulated complexes, we have found that encapsulated 4-OH-Ni-salen-Y complex has much higher magnetization than the encapsulated Ni-salen-Y complex establishing the fact that 4-OH-Ni-salen-Y complex has larger fraction of molecules in higher lying excited triplet states upon encapsulation. It is reasonable, because the bulkier 4-OH-Ni-salen-Y complex does not fit into the spherical cavity of host and hence suffers from more steric strain to accommodate itself into the cavity thus adopts more distorted geometry than encapsulated Ni-salen-Y complex.

#### **Catalytic activity and structural correlation**

Catalytic activities of the complex both in free and encapsulated states have been investigated for styrene oxidation reaction using  $H_2O_2$  as oxidant (Table 5) and Ni-salen system is employed as catalyst [1]. In this reaction, benzaldehyde is identified as major product in each of the cases whereas styrene oxide and phenyl acetaldehyde are the minor products. Nickel Schiff-base complexes are known to be less reactive than other transition metals for the oxidation reactions [33, 60]. On comparison the percentage conversion data, of both state complexes, neat complexes seems to have high conversion but there is a difference in concentration of active centers (nickel metal) as encapsulated complexes have poor loading level (concentrations of nickel metal in the encapsulated complex is 0.50 wt % and 59 wt % for the 4-OH-Ni-salen-Y and Ni-salen-Y respectively) to get maximum free zeolite surface for the reaction so relative reactivity of catalysts has been calculated in term of Turnover number, TON. It has been observed that the encapsulated complexes are more selective for benzaldehyde than their corresponding neat state [60]. Ni-salen-Y and 4-OH-Ni-salen-Y complexes in their neat form show comparatively similar reactivity for the oxidation reaction in terms of Turn Over Number (TON). Interestingly, the 4-OH-Ni-salen-Y complex

shows greater reactivity than Ni-salen-Y and UV-Vis, magnetic and TD-DFT studies evidently support the greater extent of distortion of planar geometry in 4-OH-Ni-salen-Y complex. In literature, it has been reported [61, 62] that distortion in planar complexes induces the better reactivity for the oxidation processes because, distorted planar structure induces more electropositive character on the metal, which act as more sensitive site for nucleophilic attack of the reagent. Study of relation in modified functionality and structural behaviour surely provide a new gateway to design the more effective heterogeneous catalyst which will be useful in various industrial processes.

## Conclusion

This manuscript presents detailed characterizations of complex 4-OH-Ni-salen encapsulated in zeolite -Y. The comparative morphological, spectroscopic, magnetic, catalytic and theoretical studies of both complexes have been carried out to explore the effect of the host framework on the guest complexes. XRD pattern, SEM and IR studies have indicated successful formation of the complex inside the zeolite Y cavities. Solid state UV-Visible studies have supported the complex formation in the neat and also in the encapsulated states in zeolite Y, however the d-d transitions of the encapsulated complexes are observed to be blue shifted. Interestingly, observed blue shift in d-d bands is more when compared with Ni-salen-Y TD-DFT simulated electronic spectra have supported the experimental observations and indicated that encapsulated complexes are distorted and exist in triplet states. Further the magnetic studies have presented an evident exposure about the distortion in geometry around the Ni center of encapsulated complexes, because both diamagnetic complexes show paramagnetism whereas 4-OH-Ni-salen- complex shows relatively enhanced magnetism in comparison to Ni-salen-Y complex, which again proves the effect of substituent groups in the encapsulated complex. Theoretical studies also have indicated a higher magnetic moment for 4-OH-Ni-salen-Y complex, with respect to Ni-salen-Y complex, showing good agreement with experimental magnetic behavior. The electronic, magnetic and DFT studies altogether indicate that encapsulation forces the complex to adopt a distorted geometry which drives the Ni atom out of the plane of NiN<sub>2</sub>O<sub>2</sub> moiety. This alteration in geometry lowers the energy gap between the triplet and

singlet states, which in turn, makes the energetically higher lying triplet state more accessible. Bulkier 4-OH-Ni-salen complex suffers more space constraint imposed by spherical host cavity, thus, the extent of distortion is higher, driving majority of molecules to the higher energy triplet state, eventually making it more paramagnetic than Ni-salen-Y complex. Enhanced catalytic activity of 4-OH-Ni-salen-Y complex validates the extent of distortion in adopted geometry of the guest complex as well as offers the evidences about the connection between structural and functional alterations.

### **Acknowledgements**

The authors acknowledge the Department of Science and Technology, New Delhi, for the financial support (DST Project No: SR/FT/CS-038/2010) and for the instrumental facility funded by DST-FIST, Department of Chemistry, BITS, Pilani and DST-FIST, Department of Physics, BITS, Pilani and for theoretical studies (DST Project No: SR/FT/CS-119/2010).

### **SUPPORTING INFORMATION**

Physical measurements, Theoretical methods, Synthesis methods, EDS spectra of pure zeolite Y and encapsulated Ni-salen-Y, 4-OH-Ni-salen-Y complexes, UV-Vis data of neat complex and ligands, The structure of the frontier molecular orbitals in free state and triplet encapsulated state, TD-DFT spectra for Ni-salen-Y and 4-OH-Ni-salen-Y using B3LYP and B3PW91 exchange methods.

### **AUTHOR INFORMATION**

#### **Corresponding Author**

Email: [saumi@pilani.bits-pilani.ac.in](mailto:saumi@pilani.bits-pilani.ac.in)

Contact no + 91-01596-515650

Fax no +91-(01596) 244183

#### **Present Addresses**

Dr Saumi Ray

Associate professor,

Department of Chemistry

Birla Institute of Technology and Science,

Pilani Campus, Pilani, 333031, Rajasthan. INDIA.

ACCEPTED MANUSCRIPT

**References**

- [1] A. Choudhary, B. Das, S. Ray, Enhanced Catalytic Activity and Magnetization of Encapsulated Nickel Schiff-Base Complexes in Zeolite-Y: A correlation with the Adopted Non-Planar Geometry, Dalton Trans., DOI 10.1039/C6DT03240K(2016).
- [2] P. Dutta, Zeolite guest-host interactions: Implications in formation, catalysis, and photochemistry, J. Inclusion Phenom. Mol. Recognit. Chem., 21 (1995) 215-237.
- [3] K. Balkus, Jr., A. Gabrielov, Zeolite encapsulated metal complexes, J. Inclusion Phenom. Mol. Recognit. Chem., 21 (1995) 159-184.
- [4] D. De Vos, P.P. Knops-Gerrits, R. Parton, B. Weckhuysen, P. Jacobs, R. Schoonheydt, Coordination chemistry in zeolites, J. Inclusion Phenom. Mol. Recognit. Chem., 21 (1995) 185-213.
- [5] M. Álvaro, J.F. Cabeza, A. Corma, H. García, E. Peris, Electrochemiluminescence of Zeolite-Encapsulated Poly(p-phenylenevinylene), J. Am. Chem. Soc., 129 (2007) 8074-8075.
- [6] M.L. Cano, A. Corma, V. Fornés, H. García, M.A. Miranda, C. Baerlocher, C. Lengauer, Triarylmethyl cations encapsulated within zeolite supercages, J. Am. Chem. Soc., 118 (1996) 11006-11013.
- [7] D. Peralta, G. Chaplais, A. Simon-Masseron, K. Barthelet, G.D. Pirngruber, Separation of C6 Paraffins Using Zeolitic Imidazolate Frameworks: Comparison with Zeolite 5A, Ind. Eng. Chem. Res., 51 (2012) 4692-4702.
- [8] S. Van der Perre, B. Bozbiyik, J. Lannoeye, D.E. De Vos, G.V. Baron, J.F.M. Denayer, Experimental Study of Adsorptive Interactions of Polar and Nonpolar Adsorbates in the Zeolitic Imidazolate Framework ZIF-68 via Pulse Gas Chromatography, J. Phys. Chem. C, 119 (2015) 1832-1839.
- [9] D. Jo, S.B. Hong, M.A. Camblor, Monomolecular Skeletal Isomerization of 1-Butene over Selective Zeolite Catalysts, ACS Catal., DOI 10.1021/acscatal.5b00195(2015) 2270-2274.
- [10] N.Y. Chen, W.E. Garwood, Some catalytic properties of ZSM-5, a new shape selective zeolite, J. Catal., 52 (1978) 453-458.

- [11] J.D. Rimer, M. Kumar, R. Li, A.I. Lupulescu, M.D. Oleksiak, Tailoring the physicochemical properties of zeolite catalysts, *Catal. Sci. Technol.*, 4 (2014) 3762-3771.
- [12] L. Gigli, R. Arletti, G. Tabacchi, E. Fois, J.G. Vitillo, G. Martra, G. Agostini, S. Quartieri, G. Vezzalini, Close-Packed Dye Molecules in Zeolite Channels Self-Assemble into Supramolecular Nanoladders, *J. Phys. Chem. C*, 118 (2014) 15732-15743.
- [13] L. Luo, C. Dai, A. Zhang, J. Wang, M. Liu, C. Song, X. Guo, Facile synthesis of zeolite-encapsulated iron oxide nanoparticles as superior catalysts for phenol oxidation, *RSC Adv.*, 5 (2015) 29509-29512.
- [14] V. Ramamurthy, D.F. Eaton, J.V. Caspar, Photochemical and photophysical studies of organic molecules included within zeolites, *Acc. Chem. Res.*, 25 (1992) 299-307.
- [15] T. Bein, C. Huber, K. Moller, C.-G. Wu, L. Xu, Methyltrioxorhenium Encapsulated in Zeolite Y: Tunable Olefin Metathesis Catalyst, *Chem. Mater.*, 9 (1997) 2252-2254.
- [16] M. Jaymand, Conductive polymers/zeolite (nano-)composites: under-exploited materials, *RSC Adv.*, 4 (2014) 33935-33954.
- [17] M. Álvaro, A. Corma, B. Ferrer, M.S. Galletero, H. García, E. Peris, Increasing the Stability of Electroluminescent Phenylenevinylene Polymers by Encapsulation in Nanoporous Inorganic Materials, *Chem. Mater.*, 16 (2004) 2142-2147.
- [18] C.W. Kim, H.-C. Kang, N.H. Heo, K. Seff, Encapsulating Photoluminescent Materials in Zeolites. Crystal Structure of Fully Dehydrated Zeolite Y (Si/Al = 1.69) Containing Eu<sup>3+</sup>, *J. Phys. Chem. C*, 118 (2014) 11014-11025.
- [19] V.S. Marakatti, A.B. Halgeri, Metal ion-exchanged zeolites as highly active solid acid catalysts for the green synthesis of glycerol carbonate from glycerol, *RSC Adv.*, 5 (2015) 14286-14293.
- [20] S. Li, A. Zheng, Y. Su, H. Zhang, L. Chen, J. Yang, C. Ye, F. Deng, Brønsted/Lewis Acid Synergy in Dealuminated HY Zeolite: A Combined Solid-State NMR and Theoretical Calculation Study, *J. Am. Chem. Soc.*, 129 (2007) 11161-11171.

- [21] J.H. Lunsford, W.P. Rothwell, W. Shen, Acid sites in zeolite Y: a solid-state NMR and infrared study using trimethylphosphine as a probe molecule, *J. Am. Chem. Soc.*, 107 (1985) 1540-1547.
- [22] C.R. Jacob, S.P. Varkey, P. Ratnasamy, Selective oxidation over copper and manganese salens encapsulated in zeolites, *Microporous Mesoporous Mater.*, 22 (1998) 465-474.
- [23] R.F. Parton, I.F.J. Vankelecom, M.J.A. Casselman, C.P. Bezoukhanova, J.B. Uytterhoeven, P.A. Jacobs, An efficient mimic of cytochrome P-450 from a zeolite-encaged iron complex in a polymer membrane, *Nature*, 370 (1994) 541-544.
- [24] N. Herron, A cobalt oxygen carrier in zeolite Y. A molecular "ship in a bottle", *Inorg. Chem*, 25 (1986) 4714-4717.
- [25] P.-P. Knops-Gerrits, D. De Vos, F. Thibault-Starzyk, P.A. Jacobs, Zeolite-encapsulated Mn(II) complexes as catalysts for selective alkene oxidation, *Nature*, 369 (1994) 543-546.
- [26] M. Salavati-Niasari, Host (nanocavity of zeolite-Y)/guest ([Cu([R]<sub>2</sub>-N<sub>2</sub>X<sub>2</sub>)]<sup>2+</sup> (R = H, CH<sub>3</sub>; X = NH, O, S) nanocomposite materials: Synthesis, characterization and catalytic oxidation of ethylbenzene, *J. Mol. Catal. A: Chem.*, 284 (2008) 97-107.
- [27] M. Salavati-Niasari, M. Shakouri-Arani, F. Davar, Flexible ligand synthesis, characterization and catalytic oxidation of cyclohexane with host (nanocavity of zeolite-Y)/guest (Mn(II), Co(II), Ni(II) and Cu(II) complexes of tetrahydro-salophen) nanocomposite materials, *Microporous Mesoporous Mater.*, 116 (2008) 77-85.
- [28] M. Salavati-Niasari, A. Sobhani, Ship-in-a-bottle synthesis, characterization and catalytic oxidation of cyclohexane by Host (nanopores of zeolite-Y)/guest (Mn(II), Co(II), Ni(II) and Cu(II) complexes of bis(salicylaldehyde)oxaloyldihydrazone) nanocomposite materials, *J. Mol. Catal. A: Chem.*, 285 (2008) 58-67.
- [29] M. Salavati-Niasari, M. Shaterian, M.R. Ganjali, P. Norouzi, Oxidation of cyclohexene with tert-butylhydroperoxide catalyzed by host (nanocavity of zeolite-Y)/guest (Mn(II), Co(II), Ni(II) and Cu(II) complexes of N,N'-bis(salicylidene)phenylene-1,3-diamine) nanocomposite materials (HGNM), *J. Mol. Catal. A: Chem.*, 261 (2007) 147-155.

- [30] S. Deshpande, D. Srinivas, P. Ratnasamy, EPR and Catalytic Investigation of Cu(Salen) Complexes Encapsulated in Zeolites, *J. Catal.*, 188 (1999) 261-269.
- [31] M. J. Sabater, A. Corma, A. Domenech, V. Fornes, H. Garcia, Chiral salen manganese complex encapsulated within zeolite Y: a heterogeneous enantioselective catalyst for the epoxidation of alkenes, *Chem. Commun.*, DOI 10.1039/A701337J(1997) 1285-1286.
- [32] K.O. Xavier, J. Chacko, K.K. Mohammed Yusuff, Zeolite-encapsulated Co(II), Ni(II) and Cu(II) complexes as catalysts for partial oxidation of benzyl alcohol and ethylbenzene, *Appl. Catal., A*, 258 (2004) 251-259.
- [33] M.R. Maurya, S.J.J. Titinchi, S. Chand, I.M. Mishra, Zeolite-encapsulated Cr(III), Fe(III), Ni(II), Zn(II) and Bi(III) salen complexes as catalysts for the decomposition of H<sub>2</sub>O<sub>2</sub> and oxidation of phenol, *J. Mol. Catal. A: Chem.*, 180 (2002) 201-209.
- [34] Y. Yu, J. Mai, L. Wang, X. Li, Z. Jiang, F. Wang, Ship-in-a-bottle synthesis of amine-functionalized ionic liquids in NaY zeolite for CO<sub>2</sub> capture, *Sci. Rep.*, 4 (2014).
- [35] S. Ray, S. Vasudevan, Encapsulation of Cobalt Phthalocyanine in Zeolite-Y: Evidence for Nonplanar Geometry, *Inorg. Chem.*, 42 (2003) 1711-1719.
- [36] Y. Umemura, Y. Minai, T. Tominaga, Structural Distortion of 6-Coordinated Fe(II) Complexes in Zeolite Y, *The Journal of Physical Chemistry B*, 103 (1999) 647-652.
- [37] S.K. Tiwary, S. Vasudevan, Void Geometry Driven Spin Crossover in Zeolite-Encapsulated Cobalt Tris(bipyridyl) Complex Ion, *Inorg. Chem.*, 37 (1998) 5239-5246.
- [38] K.K. Bania, R.C. Deka, Experimental and Theoretical Evidence for Encapsulation and Tethering of 1,10-Phenanthroline Complexes of Fe, Cu, and Zn in Zeolite-Y, *J. Phys. Chem. C*, 116 (2012) 14295-14310.
- [39] A. Choudhary, B. Das, S. Ray, Encapsulation of a Ni salen complex in zeolite Y: an experimental and DFT study, *Dalton Trans.*, 44 (2015) 3753-3763.
- [40] W.H. Quayle, J.H. Lunsford, Tris(2,2'-bipyridine)ruthenium(III) in zeolite Y: characterization and reduction on exposure to water, *Inorg. Chem.*, 21 (1982) 97-103.

- [41] W.H. Quayle, G. Peeters, G.L. De Roy, E.F. Vansant, J.H. Lunsford, Synthesis and spectroscopic properties of divalent and trivalent tris(2,2'-dipyridine)iron complexes in zeolite Y, *Inorg. Chem.*, 21 (1982) 2226-2231.
- [42] M. Jafarian, M. Rashvand avei, M. Khakali, F. Gobal, S. Rayati, M.G. Mahjani, DFT and Experimental Study of the Host–Guest Interactions Effect on the Structure, Properties, and Electro-Catalytic Activities of N<sub>2</sub>O<sub>2</sub>–Ni(II) Schiff-Base Complexes Incorporated into Zeolite, *J. Phys. Chem. C*, 116 (2012) 18518-18532.
- [43] K.K. Bania, D. Bharali, B. Viswanathan, R.C. Deka, Enhanced Catalytic Activity of Zeolite Encapsulated Fe(III)-Schiff-Base Complexes for Oxidative Coupling of 2-Naphthol, *Inorg. Chem.*, 51 (2012) 1657-1674.
- [44] Y. Umemura, Y. Minai, T. Tominaga, Structural Distortion of 6-Coordinated Fe(II) Complexes in Zeolite Y, *J. Phys. Chem. B*, 103 (1999) 647-652.
- [45] K.K. Bania, D. Bharali, B. Viswanathan, R.C. Deka, Enhanced Catalytic Activity of Zeolite Encapsulated Fe(III)-Schiff-Base Complexes for Oxidative Coupling of 2-Naphthol, *Inorg. Chem.*, 51 (2012) 1657-1674.
- [46] G. Ramanjaneya Reddy, S. Balasubramanian, K. Chennakesavulu, Zeolite encapsulated Ni(ii) and Cu(ii) complexes with tetradentate N<sub>2</sub>O<sub>2</sub> Schiff base ligand: catalytic activity towards oxidation of benzhydrol and degradation of rhodamine-B, *J. Mater. Chem. A*, 2 (2014) 15598-15610.
- [47] A.R. Silva, M. Martins, M.M.A. Freitas, A. Valente, C. Freire, B. de Castro, J.L. Figueiredo, Immobilisation of amine-functionalised nickel(II) Schiff base complexes onto activated carbon treated with thionyl chloride, *Microporous Mesoporous Mater.*, 55 (2002) 275-284.
- [48] J.G. Dillard, L.T. Taylor, X-Ray photoelectron spectroscopic study of schiff base metal complexes, *J. Electron. Spectrosc. Relat. Phenom.*, 3 (1974) 455-460.
- [49] L.J. Matienzo, W.E. Swartz, S.O. Grim, X-ray photoelectron spectroscopy of tetrahedral and square planar nickel(II) compounds, *Inorg. Nucl. Chem. Lett.*, 8 (1972) 1085-1091.

- [50] K.K. Bania, R.C. Deka, Zeolite-Y Encapsulated Metal Picolinate Complexes as Catalyst for Oxidation of Phenol with Hydrogen Peroxide, *J. Phys. Chem. C*, 117 (2013) 11663-11678.
- [51] B. Dutta, S. Jana, R. Bera, P.K. Saha, S. Koner, Immobilization of copper Schiff base complexes in zeolite matrix: Preparation, characterization and catalytic study, *Appl. Catal., A*, 318 (2007) 89-94.
- [52] M. Asadi, K.A. Jamshid, A.H. Kyanfar, Synthesis, characterization and equilibrium study of the dinuclear adducts formation between nickel(II) Salen-type complexes with diorganotin(IV) dichlorides in chloroform, *Inorg. Chim. Acta*, 360 (2007) 1725-1730.
- [53] R. Ganesan, B. Viswanathan, Physicochemical and Catalytic Properties of Copper Ethylenediamine Complex Encapsulated in Various Zeolites, *J. Phys. Chem. B*, 108 (2004) 7102-7114.
- [54] M.A. Siegler, M. Lutz, Ni(salen): a System That Forms Many Solvates with Interacting Ni Atoms, *Crystal Growth & Design*, 9 (2009) 1194-1200.
- [55] S. Di Bella, I. Fragala, I. Ledoux, M.A. Diaz-Garcia, P.G. Lacroix, T.J. Marks, Sizable Second-Order Nonlinear Optical Response of Donor-Acceptor Bis(salicylaldiminato)nickel(II) Schiff Base Complexes, *Chemistry of Materials*, 6 (1994) 881-883.
- [56] A. Boettcher, H. Elias, E.G. Jaeger, H. Langfelderova, M. Mazur, L. Mueller, H. Paulus, P. Pelikan, M. Rudolph, M. Valko, Comparative study on the coordination chemistry of cobalt(II), nickel(II), and copper(II) with derivatives of salen and tetrahydrosalen: metal-catalyzed oxidative dehydrogenation of the carbon-nitrogen bond in coordinated tetrahydrosalen, *Inorg. Chem*, 32 (1993) 4131-4138.
- [57] H. Yoon, C.J. Burrows, Catalysis of alkene oxidation by nickel salen complexes using sodium hypochlorite under phase-transfer conditions, *J. Am. Chem. Soc.*, 110 (1988) 4087-4089.
- [58] H.-C. Zhang, W.-S. Huang, L. Pu, Biaryl-Based Macrocyclic and Polymeric Chiral (Salophen)Ni(II) Complexes: Synthesis and Spectroscopic Study, *J. Org. Chem.*, 66 (2001) 481-487.
- [59] D.N. Stamires, J. Turkevich, Electron Spin Resonance of Molecules Adsorbed on Synthetic Zeolites, *J. Am. Chem. Soc.*, 86 (1964) 749-757.

[60] M.R. Maurya, A.K. Chandrakar, S. Chand, Zeolite-Y encapsulated metal complexes of oxovanadium(VI), copper(II) and nickel(II) as catalyst for the oxidation of styrene, cyclohexane and methyl phenyl sulfide, *J. Mol. Catal. A: Chem.*, 274 (2007) 192-201.

[61] M.M. Bhadbhade, D. Srinivas, Effects on molecular association, chelate conformation, and reactivity toward substitution in copper Cu(5-X-salen) complexes, salen<sup>2-</sup> = N,N'-ethylenebis(salicylidenediaminato), X = H, CH<sub>3</sub>O, and Cl: synthesis, x-ray structures, and EPR investigations. [Erratum to document cited in CA119(26):285036b], *Inorganic Chemistry*, 32 (1993) 6122-6130.

[62] S. Deshpande, D. Srinivas, P. Ratnasamy, EPR and Catalytic Investigation of Cu(Salen) Complexes Encapsulated in Zeolites, *Journal of Catalysis*, 188 (1999) 261-269.

**Figure captions**

**Figure 1.** Powder XRD patterns of (a) pure zeolite-Y (b) Ni exchanged zeolite-Y (c) 4-OH-Ni-salen-Y.

**Figure 2.** SEM images of (a) pure zeolite Y, (b) 4-OH-Ni-salen-Y after Soxhlet extraction.

**Figure 3.** XPS spectra of 4-OH-Ni-salen-Y complex (A) survey spectra, High resolution XPS spectra of (B) nickel (2p), (C) carbon (1s), (D) nitrogen (1s) and (E) oxygen (1s).

**Figure 4.** (A) FTIR spectra in the range of  $500\text{ cm}^{-1}$  to  $4000\text{ cm}^{-1}$  of (a) 4-OH-Ni-salen (b) 4-OH-Ni-salen-Y (c) and pure zeolite Y. (B) magnified view of IR data of (a) 4-OH-Ni-salen (b) 4-OH-Ni-salen-Y (c) and pure zeolite Y.

**Figure 5.** Solid state UV-Vis spectra in the range of 190-700 nm of (a) Ni-salen (b) 4-OH-Ni-salen (c) 4-OH-Ni-salen-Y (d) Ni-salen-Y and (e) Pure zeolite Y.

**Figure 6.** (a) Ni-salen (singlet) free state (b) 4-OH-Ni-salen free singlet state. The atoms marked by the squares define the C-Ni-C bond angle in different molecules. (c) The zeolite framework used for theoretical studies. (d) The deformation of encapsulated Ni-salen (bottom) shown with respect to its neat form (top). (e) The deformation of 4-OH-Ni-salen-Y 4-OH-Ni-salen (bottom) shown with respect to its neat form (top). (f) 4-OH-Ni-salen-Y molecule (triplet) is encapsulated within the zeolite pore.

**Figure 7.** Comparative UV-Visible data of (A) Ni-salen (B) Ni-salen-Y (C) 4-OH-Ni-salen and (D) 4-OH-Ni-salen-Y experimental data are represented by red line and TD-simulated data are represented by black vertical line.

**Figure 8.** Molar susceptibility vs temperature plots in the range of 4K-300K of (a) Ni-salen (b) Ni-salen-Y and (c) 4-OH-Ni-salen-Y.

## Figures

Figure 1

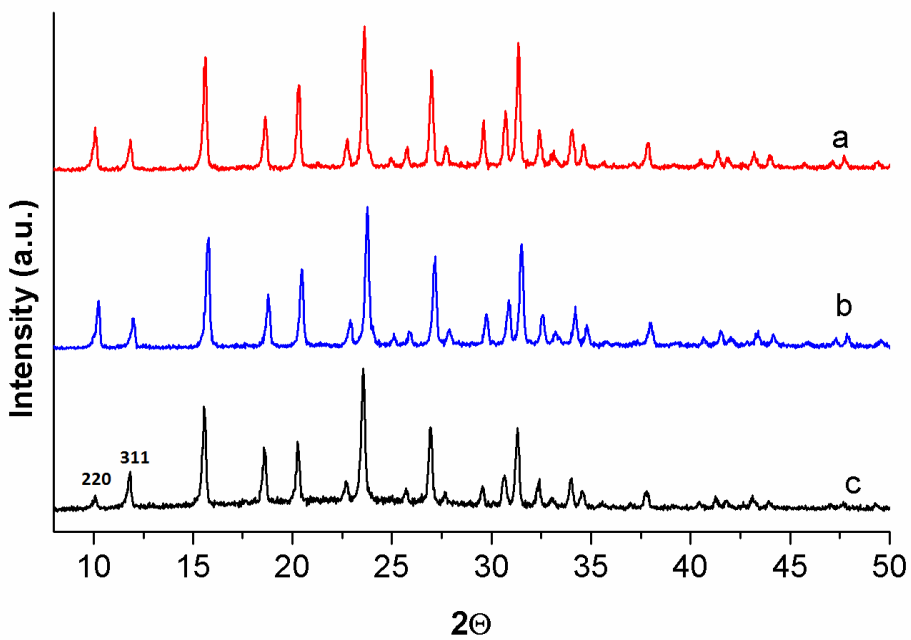
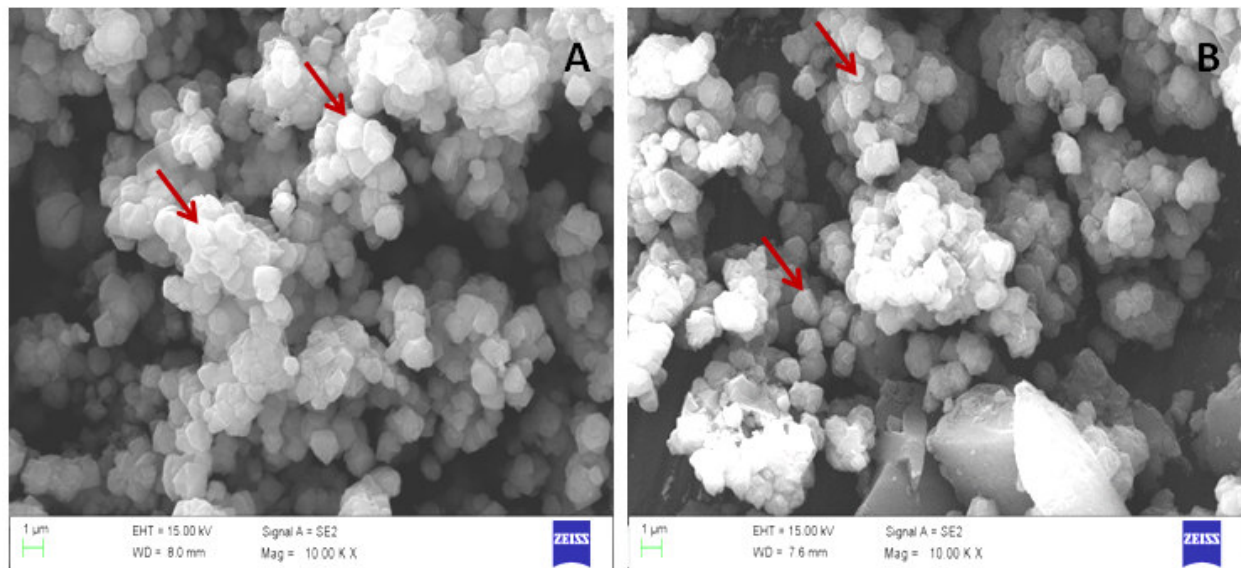


Figure 2



ACCEPTED MAN

Figure 3

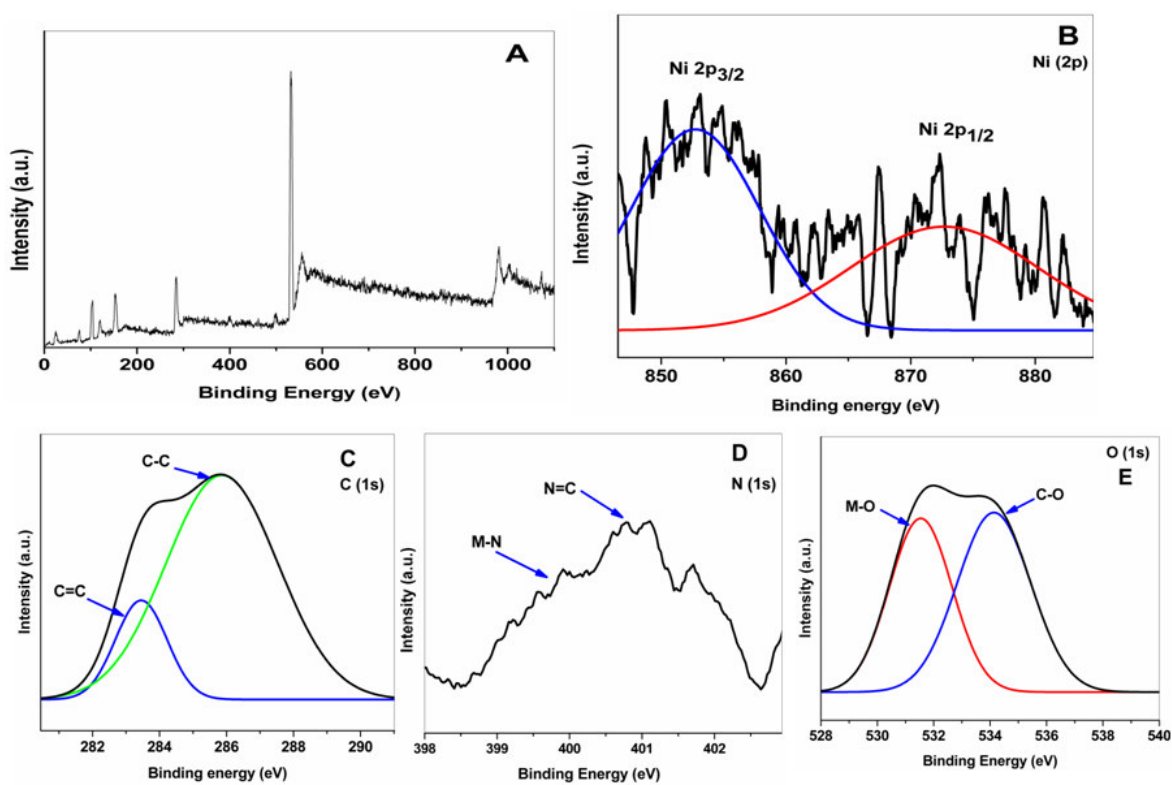


Figure 4

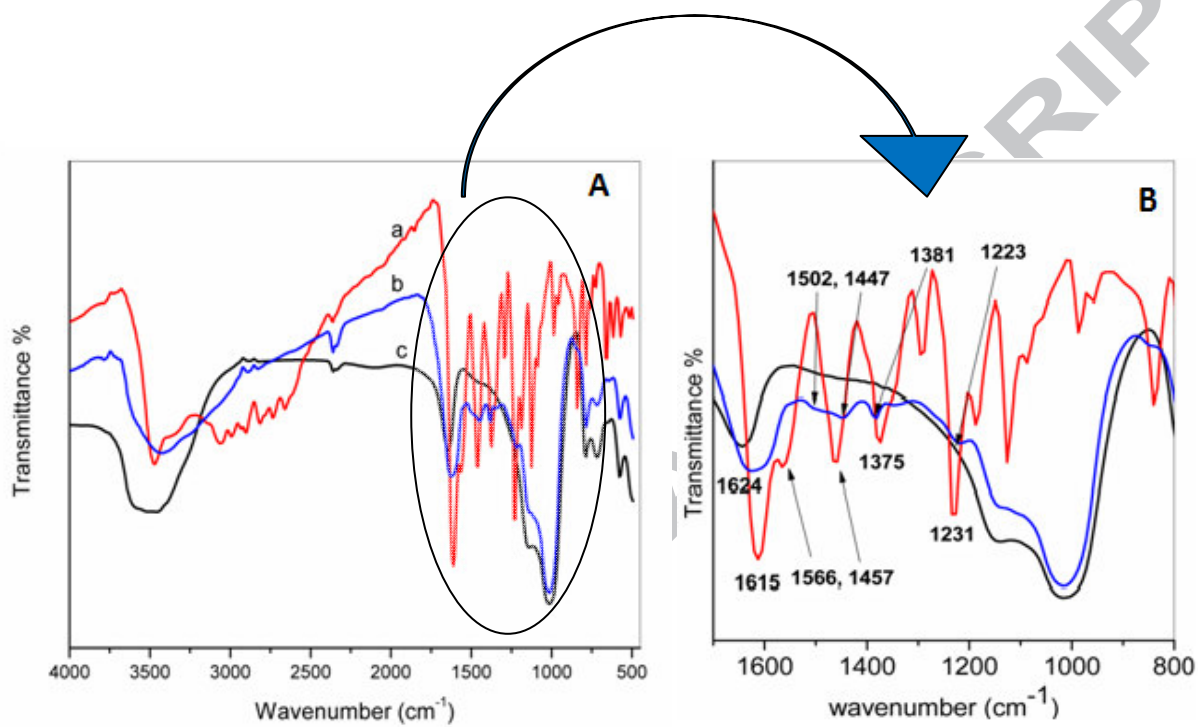


Figure 5

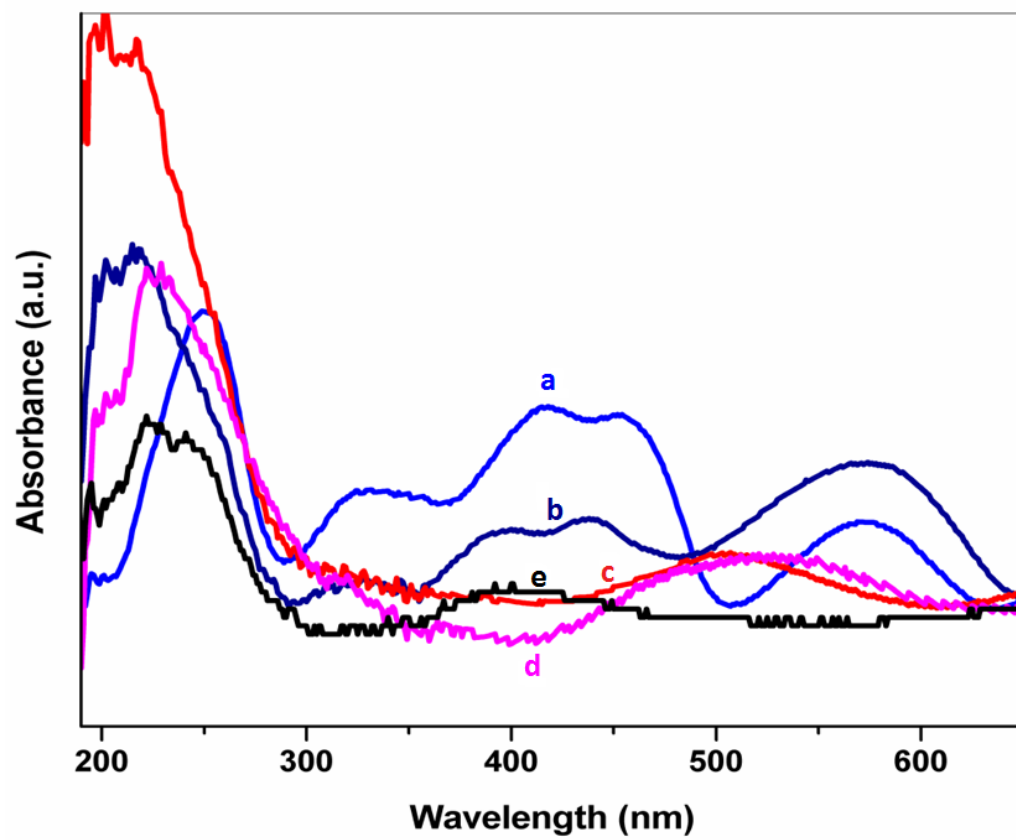
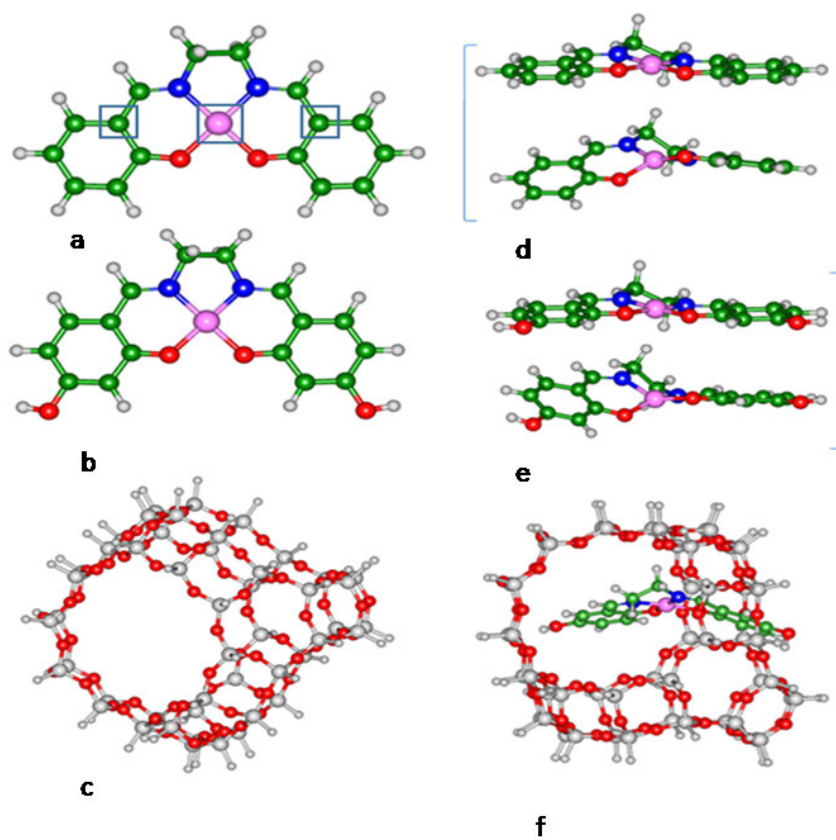


Figure 6



ACCE

Figure 7

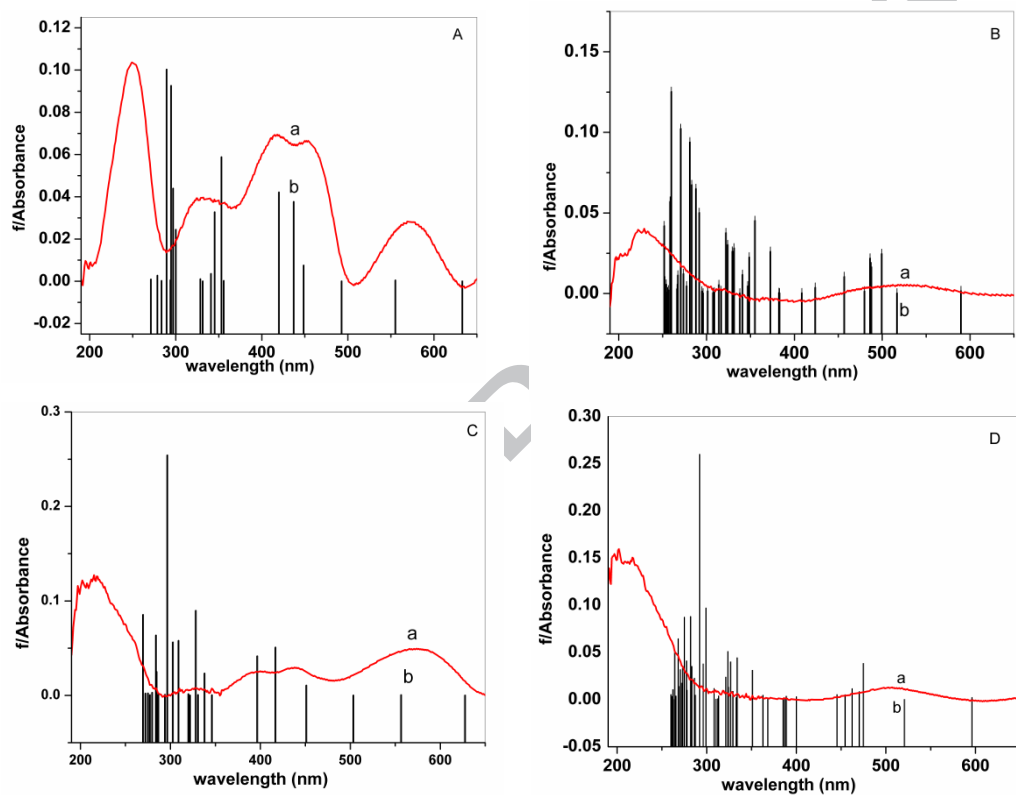
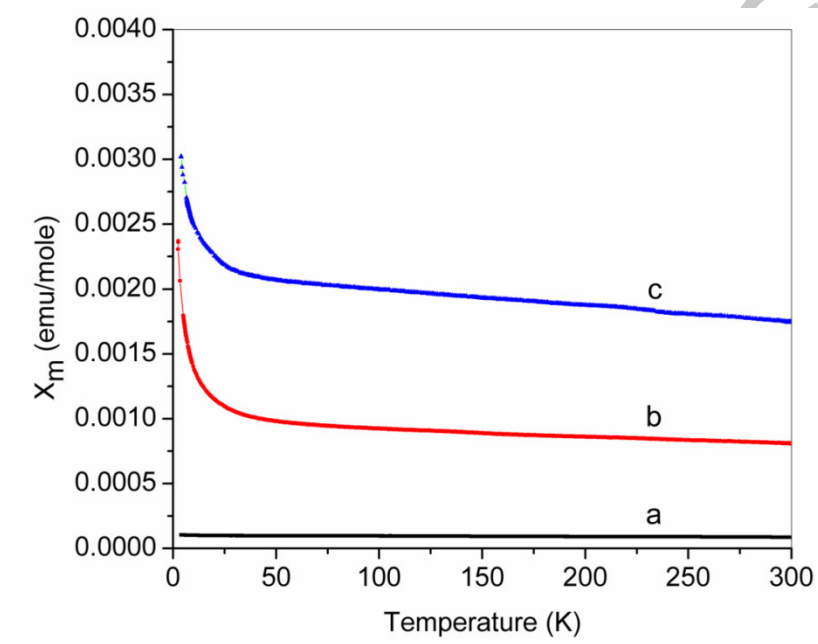


Figure 8



## Tables

Table 1 Binding energy of the neat and encapsulated complex.

Compound	Si (2p)	Al (2p)	C (1s)	N(1s)	O (1s)	Ni <sup>2+</sup> (2p)
4-OH-Ni-salen-Y	103.50	75.60	285.79, 283.43	399.67, 400.92	534.1, 531.1	853.40, 872.95

Table 2. IR spectral data ( $\text{cm}^{-1}$ ) of neat and encapsulated complexes.

S. No	Samples	(C=N) stretching	(C=C) stretching	(C-H)deformation	(C-O) stretching
1.	4-OH-Ni-salen	1613	1566, 1457	1375	1231
2.	4-OH-Ni-salen-Y	1624	1502, 1447	1381	1223

Table 3. Solid state UV-Vis spectral data of “neat” and encapsulated complexes.

<b>S. No</b>	<b>Samples</b>	$\pi-\pi^*$ <b>Transition</b>	$n-\pi^*$ <b>Transition</b>	<b>CT</b> <b>Transition</b>	$d-d$ <b>Transition</b>
<b>1.</b>	<b>Ni-salen</b>	251	323, 355	413,453	565-570
<b>2.</b>	<b>Ni-salen-Y</b>	242	320, 360		530-540
<b>3.</b>	<b>4-OH-Ni-salen</b>	241	325, 397	439	570-580
<b>4.</b>	<b>4-OH-Ni-salen-Y</b>	237	324, 382		495-505

Table 4. Important geometrical parameters and molecular orbital's for Ni-salen and 4-OH-Ni-salen in free and encapsulated case (B3LYP/6-31++G\*\*).

<b>Bond distances / angles</b>	<b>Ni-salen free singlet</b>	<b>4-OH-Ni-salen free singlet</b>	<b>Ni-salen-Y encapsulated Triplet</b>	<b>4-OH-Ni-salen-Y encapsulated triplet</b>
<b>Ni-O (A)</b>	1.85	1.85	1.88	1.89
<b>Ni-N (A)</b>	1.87	1.87	1.96	1.97
<b>O-C (A)</b>	1.30	1.29	1.30	1.29
<b>N-C(conj) (A)</b>	1.30	1.30	1.29	1.30
<b>&lt;O-Ni-N</b>	93.9	93.9	92.3	92.22
<b>&lt;C-Ni-C</b>	179.9	179.9	169.8	169.3
<b>End to end distance (Å)</b>	12.98	12.99	13.15 (twisted)	13.25
<b>HOMO (eV)</b>	-5.28	-5.26	-5.53, -5.79	-5.51, -5.79
<b>LUMO(eV)</b>	-1.83	-1.60	-1.86, -2.32	-1.66, -2.24
<b>HOMO-LUMO gap (eV)</b>	3.45	3.66	3.67, 3.47	3.85, 3.55

Table 5: Conversion of styrene after 8 hours reaction time with H<sub>2</sub>O<sub>2</sub> as oxidant.

S. No	Complexes	% Conversion	TON	Selectivity for Benzaldehyde (%)	Selectivity for Styrene Oxide (%)
1	Ni-salen[1]	14	109	52	48
2.	Ni-salen-Y[1]	5	90	97	3
3	4-OH-Ni-salen	12	101	70	30
4	4-OH-Ni-salen-Y	11	235	88	12

Reaction conditions - Styrene: 1.56 g, 15 mmol, H<sub>2</sub>O<sub>2</sub>: 3.40 g, 30 mmol, acetonitrile 15 ml, temperature 80<sup>0</sup> C, and catalyst (0.075 g for encapsulated complexes and 0.006 g for neat complexes)TON (turn over number): mole of substrate converted per mole of metal center (encapsulated complexes).

## Encapsulated Schiff Base Nickel Complex

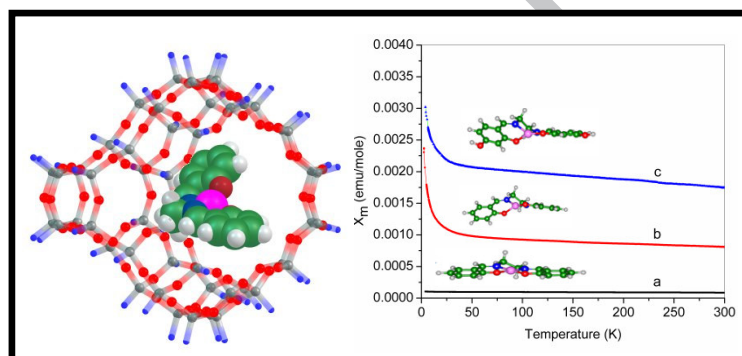
in Zeolite Y: Correlation Between Catalytic Activities and Extent of Distortion Supported by Experimental  
and DFT Studies

## TOC

Archana Choudhary<sup>a</sup>, Bidisa Das<sup>b</sup> and Saumi Ray<sup>\*a</sup>

<sup>a</sup> Birla Institute of Technology and Science, Pilani, Rajasthan 333031.

<sup>b</sup> Indian Association for the Cultivation of Science, Jadavpur, Kolkata 700032.



**Highlights:** It is observed that planar Ni (II)–Schiff base complexes with N, N'-bis(4-hydroxy salicylidene)ethylenediamine (4-OH-salen) when encapsulated in the supercage of zeolite Y, the complex adopts non-planar geometry. The detailed characterization studies of the 4-OH-Ni-salen complex when compared with that of Ni-salen complex encapsulated in zeolite Y (Ni-salen-Y)[1] suggest that the 4-OH-Ni-salen complex undergoes more distortion in order to accommodate itself inside the supercage of zeolite-Y. Optical spectroscopic studies show relatively more blue shifted and intensified d-d transition for 4-OH-Ni-salen complex after encapsulation. We also report the catalytic activities and enhanced magnetization of encapsulated complex.